Using a Modified Bréguet Range Equation to Assess the Feasibility of Hybrid Regional Aircraft Designs

James Atkinson – May 2025

List of Symbols and Abbreviations

MTOW	Maximum Take-off Weight
OEW	Operating Empty Weight
SAF	Sustainable Aviation Fuel
PSFC	Power Specific Fuel Consumption
PFS	Percent Fuel Saving
R	Range
g	Acceleration due to Gravity ($9.81\ m\ s^{-2}$)
C_L/C_D	Lift/Drag Ratio
E	Energy
m	Mass
η	Efficiency
e	Gravimetric Energy Density
φ	Degree of Hybridisation

Abstract

A series of equations for the range and mass of fuel consumed for both conventional and series hybrid aircraft are derived and presented. Parameters from three real world aircraft, the Cessna Caravan 208, the Saab 340B and the ATR 72-600, are used as the basis for comparing fuel consumption at different ranges and at different Maximum Take-off Weights.

Increasing the MTOW generally leads to an increase in fuel saving for a given range as more battery energy can be stored. This follows a law of diminishing returns, however. The relationship also breaks down for lower battery gravimetric energy densities at a certain intersection point for lower battery gravimetric energy densities. This point can lie well below the maximum range of the conventional aircraft and usually represents almost no fuel saving, which is important to consider when designing an aircraft with a certain range in mind.

Results and limitations of the model are discussed as well as potential opportunities and challenges associated with the adoption of hybrid aircraft in industry.

Introduction

Motivation

In recent years, hybrid aircraft have been gaining increasing popularity in the bid to decarbonise the civil aviation sector. Using solely batteries allows aircraft to hypothetically achieve net zero emissions with higher plug-to-wake efficiency than other alternative fuels derived from electrical power such as liquid hydrogen [18] or Power-to-Liquid Sustainable Aviation Fuel [19] due to the comparatively low number of conversion steps from mains power to charging.

However, battery electric aircraft are typically very limited in range due to the low gravimetric energy density of batteries compared to jet fuel. In order to combat this deficit, hybridisation has been proposed as a potential solution to the problem. Using both batteries and traditional jet fuel or SAF allows for the improved carbon footprint and energy efficiency of electricity as well as the higher energy density of jet fuel.

Hybrid aircraft are garnering interest from industry. Airbus, Daher and Safran explored the potential of hybrid aircraft in their EcoPulse project which completed flight testing in July 2024 [22]. Swedish company Heart Aerospace is also proposing a hybrid aircraft design, planning to have its ES-30 regional aircraft certified by 2029 [23].

Government funded research projects have also explored hybridisation as an avenue for at least partial decarbonisation. The Hybrid Electric Regional Architecture Project, funded by the European Union, has produced various papers on the topic, primarily focusing on mathematical modelling [21]. The German Aerospace Research Centre (DLR)'s EXACT program has also conducted similar work with more of a focus on multidisciplinary design optimisation, producing various low or no emission airliner concepts at the regional and narrowbody scale [20]. Their Plug-in Hybrid Electric Propulsion concept proposes a 70% reduction in emissions compared to current aircraft of its size [20].

This paper sets out to derive a Bréguet-style range equation to act as a basis for comparison between current aircraft serving the sub-regional to regional sectors. While it is not the first paper to use real aircraft as a baseline for parameters, for example, Elmousadik et al. [24] make use of the Pilatus PC-12 as their reference, the selection of 3 aircraft of varying size provides valuable comparative insight.

Parallel vs Series Configurations

Hybrid aircraft are most commonly designed with either a series or parallel configuration [1]. In a series configuration, electric motors are what drive the shaft of the propeller at all times. The energy from the fuel must first be converted into electrical energy by means of a generator before being fed to the motors, and the energy in the battery can be used more or less directly [1], [25].

In a parallel architecture a gearbox is connected to the propellors and can be driven by either a fuel-powered turbine, a battery-powered electric motor or both at the same time [1], [25].

This paper examines a series hybrid design.

Trends in Battery Technology

The adoption of lithium ion batteries in aerospace has typically been avoided due to their poor gravimetric energy density compared to fuel. However, recent advancements in the field of battery chemistry could see significant improvements in energy density over the coming years.

For example, there are various chemistries being explored that could increase the current value of around 280 Wh kg^{-1} to the mid hundreds [26]. One particularly promising development is that of solid state batteries where the electrolyte is solid rather than a gel structure. This comes with the advantage of improved safety and energy density [26].

Some companies have promised to deliver batteries with exceptional gravimetric energy densities such as CATL which has claimed to have developed a battery with an energy density of 500 Wh kg^{-1} [27] and Wright Electric which is planning to release a battery with an energy density of 800 Wh kg^{-1} [28].

Factoring in the various possible trajectories for gravimetric energy density over the coming decade, for this paper, separate figures at 300, 500, 700 and 900 Wh kg^{-1} are plotted for each aircraft.

Derivation of Series Hybrid Range Equation

Total Range

We will assume that we begin the flight by first consuming all of the fuel and then moving to battery power.

$$R = \int_0^t V dt = \int_0^t \frac{TV}{T} dt = \int_0^t \frac{\eta_{tot} P_{drawn}}{T} dt$$

For steady level flight, Thrust = Drag ($T = D$) and Lift=Weight ($L = mg$), thus $mg \cdot \frac{D}{L} = T = mg\frac{C_D}{C_L}$

Assuming the Lift Drag ratio and total energy source to useful power efficiency remains constant throughout flight (realistically this would vary at different points in the flight).

$$R = \int_0^t \frac{\eta_{tot} P_{drawn}}{mg\frac{C_D}{C_L}} dt = \frac{\eta_{tot}}{g}\frac{C_L}{C_D}\int_0^t \frac{P_{drawn}}{m} dt$$

In the fuel powered regime

$$R_{fuel} = \frac{\eta_{tot}}{g}\frac{C_L}{C_D}\int_0^t \frac{P_{drawn}}{m} dt = \frac{\eta_{fuel\ chain}}{g}\frac{C_L}{C_D}\int_0^t \frac{e_{fuel}\dot{m}_{fuel}}{m} dt$$

Where e_{fuel} is the gravimetric energy density of the fuel and $\dot{m}_{fuel}$ is the fuel mass flow rate.

$$\frac{dm}{dt} = -\dot{m}_{fuel}$$

And so, because e_{fuel} is constant,

$$R_{fuel} = -\frac{\eta_{fuel\ chain}}{g}\frac{C_L}{C_D} e_{fuel}\int_0^t \frac{-\dot{m}_{fuel}}{m} dt$$

And thus the integral now takes the standard form $\int_0^x \frac{f'(x)}{f(x)} dx = \ln|f(x)| - \ln|f(0)|$

$$R_{fuel} = -\frac{\eta_{fuel\ chain}}{g}\frac{C_L}{C_D} e_{fuel} \ln\left|\frac{m(t)}{m(0)}\right|$$

$$R_{fuel} = \frac{\eta_{fuel\ chain}}{g}\frac{C_L}{C_D} e_{fuel} \ln\left|\frac{m(0)}{m(t)}\right|$$

And, assuming the weight of the fuel has been fully exhausted

$$R_{fuel} = \frac{\eta_{fuel\ chain}}{g}\frac{C_L}{C_D} e_{fuel} \ln\left|\frac{m_{oe} + m_{bat} + m_{pay} + m_{fuel}}{m_{oe} + m_{bat} + m_{pay}}\right|$$

Operating in the battery electric regime, m does not change. Therefore

$$R_{elec} = \frac{\eta_{bat\ chain}}{g}\frac{C_L}{C_D}\frac{1}{m}\int_0^t P_{drawn} dt$$

$$R_{elec} = \frac{\eta_{bat\ chain}}{g}\frac{C_L}{C_D}\frac{E_{bat}}{m_{oe} + m_{bat} + m_{pay}}$$

$$R_{elec} = \frac{\eta_{bat\ chain}}{g}\frac{C_L}{C_D}\frac{e_{bat} m_{bat}}{m_{oe} + m_{bat} + m_{pay}}$$

Leaving in terms of m_{fuel} and m_{to} (MTOW)

$$R_{fuel} = \frac{\eta_{fuel\ chain}}{g}\frac{C_L}{C_D} e_{fuel} \ln\left|\frac{m_{to}}{m_{to} - m_{fuel}}\right|$$

$$R_{elec} = \frac{\eta_{bat\ chain}}{g}\frac{C_L}{C_D}\frac{e_{bat} m_{bat}}{m_{to} - m_{fuel}}$$

The total range can be expressed as follows:

$$R_{tot} = \frac{1}{g}\frac{C_L}{C_D}\left(\eta_{fuel\ chain} e_{fuel} \ln\left(\frac{m_{to}}{m_{to} - m_{fuel}}\right) + \eta_{bat\ chain}\frac{e_{bat} m_{bat}}{m_{to} - m_{fuel}}\right)$$

MTOW will always be higher than MTOW – fuel mass so the pipe brackets are redundant.

Mass of Fuel Consumed

In order to calculate m_{fuel} in terms of the Degree of Hybridisation, φ

$$\varphi = \frac{E_{bat}}{E_{bat} + E_{fuel}}$$

Other papers, such as Batra et al. [1] define the Degree of Hybridisation in terms of power consumption and factor in efficiencies of each power production regime at the point where the Degree of Hybridisation is calculated. As we are dealing with overall energy consumption, the author of this paper saw it fit to factor in efficiency later in the process, however this may be a point of contention.

$$\varphi = \frac{m_{bat}e_{bat}}{m_{bat}e_{bat} + m_{fuel}e_{fuel}}$$

$$\varphi\left(m_{bat}e_{bat} + m_{fuel}e_{fuel}\right) = m_{bat}e_{bat}$$

$$(1-\varphi)m_{bat}e_{bat} = \varphi m_{fuel}e_{fuel}$$

At this point, it is useful to leave the mass of fuel consumed in terms of a total mass dedicated to energy storage. This mass will be the sum of the fuel and battery masses at take-off and can therefore be written in terms of the MTOW, OEW and payload mass:

$$m_{energy} = m_{to} - m_{oe} - m_{pay} = m_{bat} + m_{fuel}$$

Rewriting the previous equation in terms of the mass of energy:

$$(1-\varphi)(m_{energy} - m_{fuel})e_{bat} = \varphi m_{fuel}e_{fuel}$$

$$(1-\varphi)\left(m_{energy}\right)e_{bat} = m_{fuel}(\varphi e_{fuel} + (1-\varphi)e_{bat})$$

$$m_{fuel\,(hybr\ \ )} = \frac{(1-\varphi)\left(m_{energy}\right)e_{bat}}{\varphi e_{fuel} + (1-\varphi)e_{bat}}$$

In order to figure out how much fuel a conventional aircraft equivalent would burn along the same total range, we need to calculate the mass of fuel as a function of range.

For conventional aircraft, $\eta_{fuel\ chain}e_{fuel}$ is written in terms of the Power Specific Fuel Consumption as $\frac{\eta_{prop}}{f_p}$ where f_p is the PSFC [9]. Our equation thus becomes

$$R_{conv} = \frac{\eta_{prop}}{f_p g}\frac{C_L}{C_D}\ln\left(\frac{m_{to(conv)}}{m_{to(conv)} - m_{fuel(conv)}}\right)$$

$$R_{conv}\frac{C_D}{C_L}\frac{f_p g}{\eta_{prop}} = \ln\left(\frac{m_{to(conv)}}{m_{to(conv)} - m_{fuel(conv)}}\right)$$

$$\exp\left(R_{conv}\frac{C_D}{C_L}\frac{f_p g}{\eta_{prop}}\right) = \frac{m_{to(conv)}}{m_{to(conv)} - m_{fuel(conv)}}$$

$$\exp\left(-R_{conv}\frac{C_D}{C_L}\frac{f_p g}{\eta_{prop}}\right) = \frac{m_{to(conv)} - m_{fuel(conv)}}{m_{to(conv)}}$$

$$m_{to}\exp\left(-R_{conv}\frac{C_D}{C_L}\frac{f_p g}{\eta_{prop}}\right) = m_{to(conv)} - m_{fuel(conv)}$$

$$-m_{fuel(conv)} = m_{to}\left(\exp\left(-R_{conv}\frac{C_D}{C_L}\frac{f_p g}{\eta_{prop}}\right) - 1\right)$$

$$m_{fuel\,(conv)} = m_{to\,(conv)}\left(1 - \exp\left(-\frac{g f_p R_{conv}}{\frac{C_L}{C_D}\eta_{prop}}\right)\right)$$

Finally, in order to calculate the Percent Fuel Saving we use the following formula:

$$P.F.S. = \left(1 - \frac{m_{fuel\,(hybrid)}}{m_{fuel\,(conv)}}\right) \times 100\%$$

Methodology

Real world data for 3 sub-regional/regional aircraft was collected to calculate their respective Bréguet Ranges, namely the Cessna 208 Caravan, the Saab 340B and the ATR 72-600 from their respective manufacturer brochures [6], [7] and [8]. For the Caravan, the brochure indicates a varying maximum number of occupants between 10 and 14 and so, estimating 100 kg per passenger with baggage, 1200 kg of payload was estimated for the maximum. Their respective MTOW, OEW and maximum payloads were compiled into MATLAB arrays so that repetitive calculations could be carried out.

	OEW/kg	MTOW/kg	Payload/kg
Cessna Caravan 208	2145	3629	1200
Saab 340B	8620	13155	3298
ATR 72-600	13600	23000	7400

Power Specific Fuel Consumption data for all aircraft was extracted from a website hosted by Purdue University [2] and then converted to $\text{kgs}^{-1}\text{W}^{-1}$

	PSFC/ $\text{lb hp}^{-1}\text{ hr}^{-1}$	PSFC/ $\text{kg s}^{-1}\text{ W}^{-1} \times 10^{-8}$
Cessna Caravan 208	0.659	11.1348
Saab 340B	0.461	7.7893
ATR 72-600	0.468	7.9076

Lift/Drag ratio data was retrieved from different sources for each aircraft. For the Cessna Caravan, the peak Lift/Drag ratio was estimated from the peak value of Figure 6 of Yusuf et al. [3]. For the Saab 340, the data was estimated from Figure 9d of Sahin et al. [4] using the peak value of the DATCOM curve. For the ATR72, data was extracted from page 17 the Aerospace Technology Institute's FlyZero report [5].

	L/D
Cessna Caravan 208	13.5
Saab 340B	14
ATR 72-600	16.8

Efficiency data for the hypothetical hybrid design were extracted from Batra et al. [1] as follows:

η_{prop}	0.8
$\eta_{turbine}$	0.35
$\eta_{generator}$	0.98
η_{motor}	0.9

$\eta_{gearbox}$	0.95
$\eta_{fuel\ chain}$	$\eta_{turbine}\eta_{generator}\eta_{gearbox}\eta_{motor}\eta_{prop}$
$\eta_{bat\ chain}$	$\eta_{gearbox}\eta_{motor}\eta_{prop}$

After deriving the sets of equations, an attempt to use MATLAB's Optimisation Toolbox was carried out, however the optimal Degree of Hybridisation for fuel saving failed to converge. To solve this issue, a separate script was written to generate surface plots to visualise the geometry of the problem.

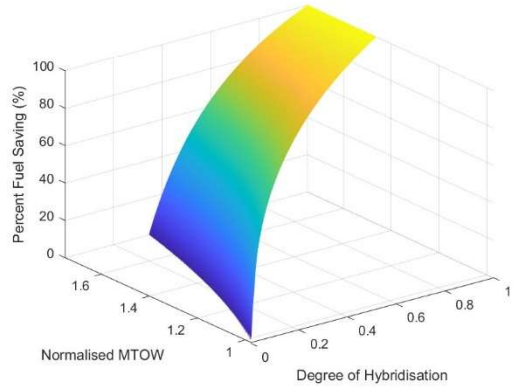

Figure 1: Percent Fuel Saving for a Cessna Caravan 208 as a function of Normalised MTOW and Degree of Hybridisation. Battery Energy Density = 500 Wh/kg, Range Requirement = 500 km.

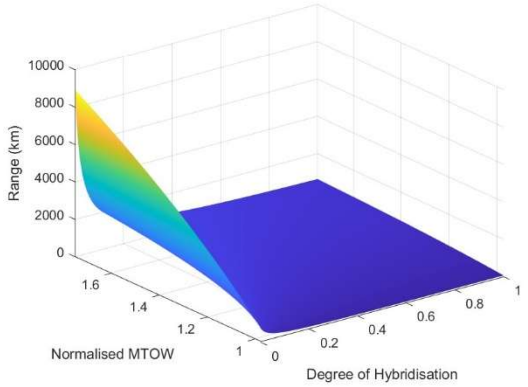

Figure 2: Range as a function of Normalised MTOW and Degree of Hybridisation. Battery Energy Density = 500 Wh/kg.

In order to cope with the poor energy density of the battery compared to the fuel, the Mass of Energy must increase. This in turn necessitates an increase in the Maximum Take-off Weight, which is measured in multiples of the original MTOW using the Normalised MTOW.

In Figure 1, all points where the Percent Fuel Saving is negative, or any points that do not meet the range requirement are excluded from the graph. This leads to a vertical shortening and a cut from the right hand side respectively.

What we can then see is that increasing the Mass of Energy (and thus the MTOW) allows us to achieve higher Degree of Hybridisation and thus greater fuel saving for a given range because we can accommodate more battery energy, offsetting fuel.

Figure 2 shows, rather intuitively, that increasing the proportion of battery energy for a given MTOW decreases the range the aircraft can fly, but range increases regardless as the MTOW is increased.

Once these plots were created, it became clear that a certain method of solving for the optimal Degree of Hybridisation would be appropriate, namely a binary search.

Because the function is monotonic (i.e. only ever increasing or decreasing) in terms of both range and Degree of Hybridisation, increasing the Degree of Hybridisation at a given MTOW *always* leads to an increase in Percent Fuel Saving at the expense of decreasing the range. The value that saves the most fuel is thus the one that only just meets the requirement for range.

The way we go about finding this value is by performing a binary search and iterating to converge onto the boundary between feasibility and infeasibility.

This works by selecting an upper bound (initially 1), a lower bound (initially 0) and calculating their mean which acts as the midpoint. If the Degree of Hybridisation at the midpoint is too high to satisfy the range requirement, the upper bound is set to the midpoint and the midpoint is then recalculated. This is because the Degree of Hybridisation can be no higher than this value, as all higher values are infeasible.

Likewise, if the range at the midpoint is higher than the requirement, then we know we could save more fuel by increasing the Degree of Hybridisation, and so the lower bound is set to the midpoint and the midpoint is recalculated.

The algorithm was implemented using 16 iterations at each new range point. For each range point, the mass of fuel consumed by a conventional equivalent aircraft operating at maximum payload was also calculated to compare to the mass of fuel consumed by the hybrid by calculating the Normalised Fuel Consumption. Subtracting from 1 and multiplying by 100, the percentage fuel saving could also be calculated.

The range points spanned from 0 to the maximum range of the conventional equivalent operating at maximum fuel and maximum payload.

12 separate figures were produced, with 3 aircraft and 4 values of the Battery Specific Energy Density. The Battery Specific Energy Density also made use of a 0.8 correction factor, as charging or discharging lithium ion batteries close to their maximum or minimum State of Charge can be detrimental to their longevity [29], [30].

Results

The figures below show the highest Percentage Fuel Saving for each given range when the aircraft is operating at maximum payload. 5 curves on each figure correspond to the MTOW being multiplied by 1, 1.25, 1.5, 1.75 and 2 respectively, allowing for more mass to be dedicated to energy storage.

The battery energy density ranges from 300 Wh/kg to 900 Wh/kg. The range starts at 0 and ends at the maximum Bréguet Range of the conventional aircraft operating at maximum payload.

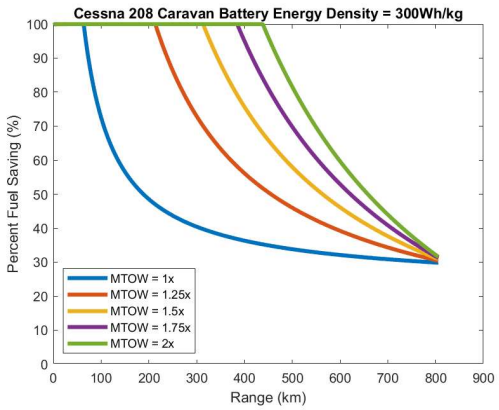

Figure 3a

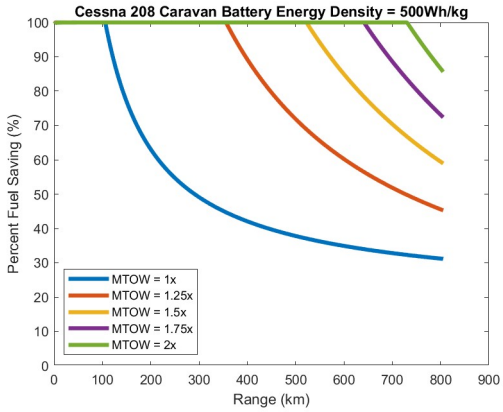

Figure 3b

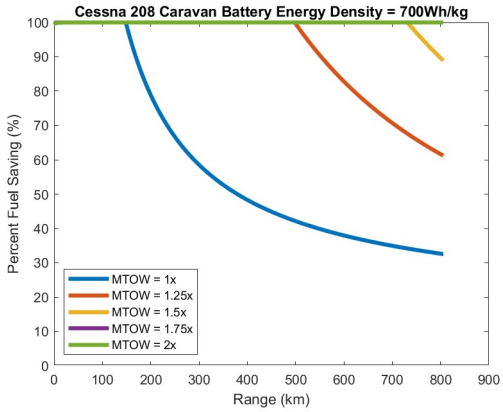

Figure 3c

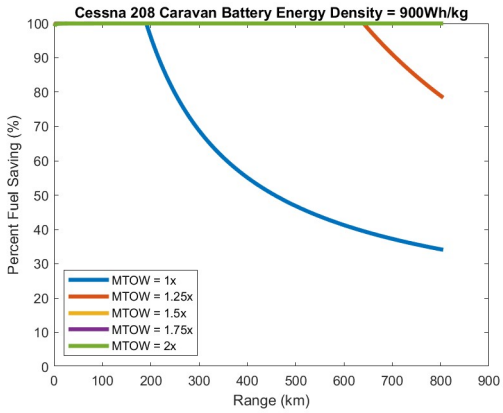

Figure 3d

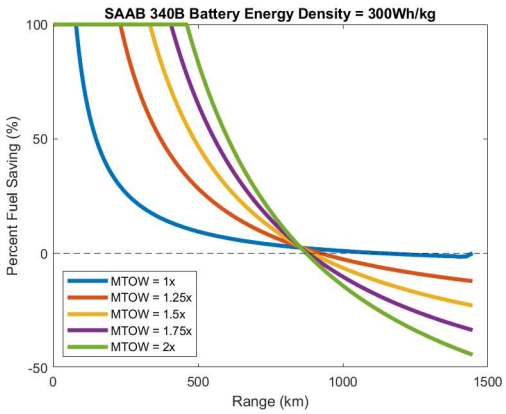

Figure 4a

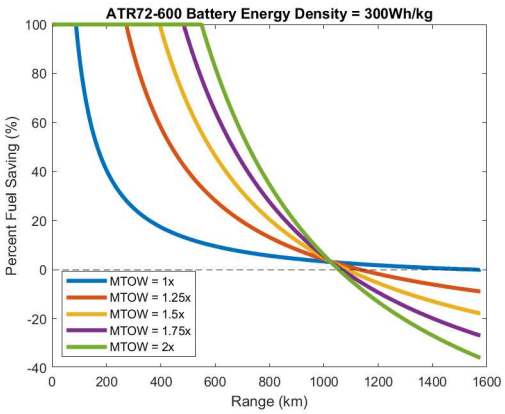

Figure 5a

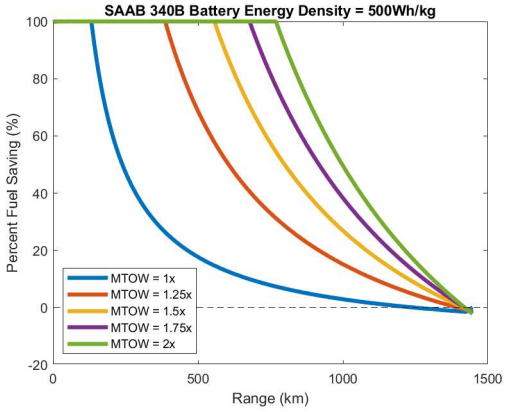

Figure 4b

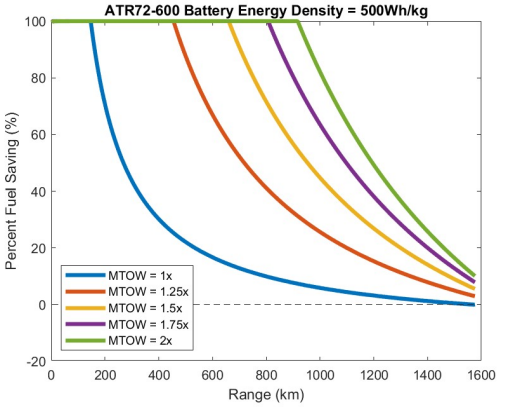

Figure 5b

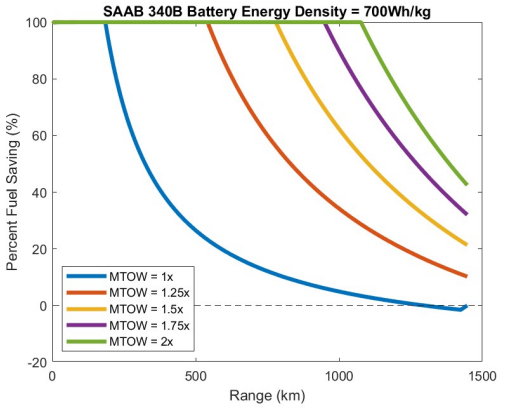

Figure 4c

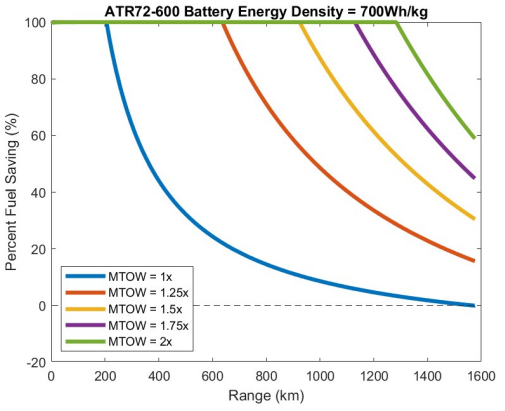

Figure 5c

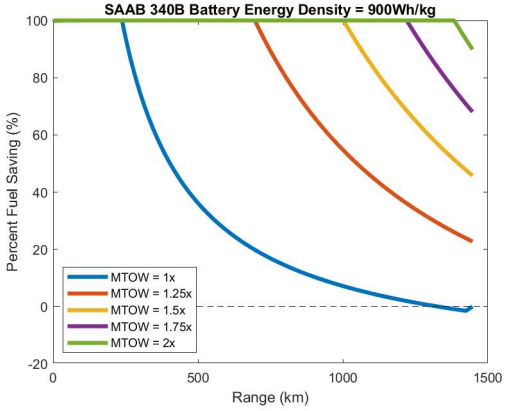

Figure 4d

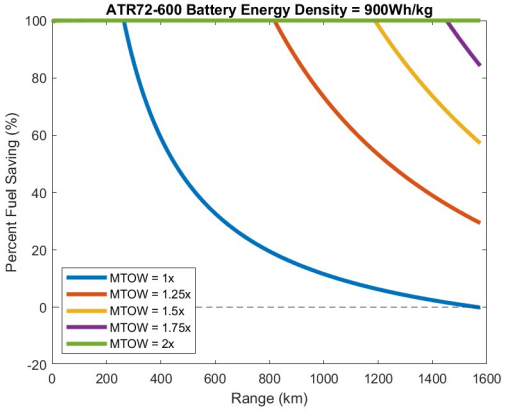

Figure 5d

Discussion

A few interesting things can be noted from the above figures. One is the region to the left of each curve where the aircraft can be fully battery powered, denoted by the graph being flat at 100% fuel saving and then decreasing at the end of the region.

In some cases, particularly noticeable for the Caravan, the lines at higher MTOWs never descend up to the maximum range of the conventional equivalent if the battery energy density is high enough. This means that with a high enough energy density, the aircraft could go fully electric up to its original maximum range.

Another observation is that the distance between lines grows smaller even if the MTOW is increased linearly. This suggests that there is a law of diminishing returns with regards to the effect that increasing the MTOW has on allowing higher Degrees of Hybridisation.

This conclusion is particularly important, as it could guide design decisions with regards to how much more load the structure needs to be able to handle. Increasing the MTOW from 1x to 1.25x may be a trade-off worth executing due to the potential fuel savings, however 1.25x to 1.5x may be more questionable, and anything above 1.5x would likely be too infeasible to be worth exploring.

As the energy density of the battery increases, the distance between lines does so as well and so this also factors into the trade-off between increasing MTOW and decreasing fuel burn.

Another interesting characteristic of the curves is that they seem, at least at a distance, to intersect at a single point. While it's unclear if the curves intersect exactly at one point (zooming in in MATLAB reveals they don't, but this could be a function of the way MATLAB plots discrete data), the physical significance of this intersection point is that it represents where the trade-off between increasing the MTOW and increasing the fuel saving breaks down and reverses.

Take Figure 5a for example. Just after 1000 km of range, the curves intersect at what seems to be a single point, meaning that at that range, no matter what the MTOW is, the same fuel saving is achieved.

To the right of this point the MTOW=1 curve actually performs the best, achieving fuel savings no less than 0%, however the others perform worse than the conventional, achieving negative fuel savings, meaning they are burning more fuel than a conventional aircraft would.

The intersection point lies close to the PFS=0% line, and so realistically, hybrid aircraft should not be designed for ranges to the right of this point. This point only becomes visible for $300\ \mathrm{W\,h\,kg^{-1}}$ battery energy density. This is alarming however, as for both Figure 4a and Figure 5a, the intersection lies well below the conventional range.

Conclusion

Limitations of the Model

There are a few important limitations of the model used in this paper that require addressing.

The first is the fact that the Bréguet Range Equation (as well as the equation derived in this paper) require the assumption of steady level flight, as well as require that certain parameters remain constant throughout the flight.

This means that the aircraft is assumed to start and end its flight in cruise, which doesn't factor in the fact that different phases of flight have their own unique power requirements.

For example, a challenge for hybrid aircraft is designing electrical systems that can handle the power requirements of the aircraft at take-off. The ATR72-600, for example, makes use of a powertrain capable of just over 2 MW of shaft power [8]. Motors capable of such powers are not currently commercially available, however some notable companies such as Wright Electric [31] and ZeroAvia [32] have either demonstrated such technology in-house or have plans to commercialise it.

However, on the other hand, the model may also neglect the fact that for shorter flights, taxiing makes up a more significant proportion of total used energy [34], and this phase of flight could be performed much more efficiently if the landing gear were directly driven by an electric motor as opposed to via a propeller [33].

Another limitation is the assumption of certain parameters remaining constant throughout flight, namely the various efficiencies, in particular the propeller efficiency, as well as the Lift/Drag ratio.

These parameters will realistically vary during the mission. For example, the propeller efficiency is a function of the advance ratio which is in turn a function of the airspeed [9] and so pulling them out of the integral may not be valid for a more accurate model of how these parameters change with time.

In order to capture this more nuanced behaviour, expressions for each parameter could be derived from experimental data and curve fitting or interpolation could be used to express them as a function of other variables.

A numerical methods approach could then be used to evaluate the integral as the parameters change across time. The various stages of flight could also be more accurately modelled, allowing for a more realistic picture of how the aircraft consumes energy throughout the mission.

A distinct advantage of this approach is that it, in turn, can be used to figure out the optimal flight profile for a given design [10]. This analysis may allow for hybrid aircraft designs to achieve greater performance than they otherwise would have if they were to follow the typical flight profile of a conventional aircraft.

Another important consideration is that the above results do not factor in reserve fuel/battery power for diversions or go arounds in case of emergencies. Reserve fuel in these cases is calculated on a mission by mission basis and depends on factors such as weather conditions and the proximity of alternate aerodromes [11].

Potential Limitations of Hybrid Aircraft

Finally, a large focus of this paper has been on the relationship between Maximum Take-off Weight and the potential for fuel saving, however it is important to address the notable structural and operational trade-offs that hybrid aircraft pose.

Firstly the structure needs to be made stronger to withstand increasing static loads as well as dynamic loads, notably upon landing. Because the mass of the aircraft decreases less between take-off and landing as the Degree of Hybridisation increases, this means that the aircraft must withstand heavy landings close to the MTOW.

Such landings could induce structural damage without proper reinforcement, however this is likely to increase the Operating Empty Weight, something not factored in by the model. This could lead to somewhat of a positive feedback loop.

On a more positive note, the aircraft analysed in this paper were all introduced in the 1980s before certain developments in materials science, notably the widespread adoption of composite materials in aerospace. These offer a potential avenue to offset the increase in Operating Empty Weight due to their high specific strength.

However the most important material property in this case would be impact resistance/fracture toughness. Carbon Fibre Reinforced Polymers, widely used in aerospace, exhibit relatively poor fracture toughness, however this can be improved by adding other fibres to the material to make a hybrid composite [12].

Another important consideration when it comes to heavy landings is how the increased load might lead to accelerated degradation of the runway surface [35]. If heavier hybrid aircraft were to be adopted at scale, the increased runway maintenance costs may prove burdensome for the small regional airports where they would typically operate. The installation of charging infrastructure and the implementation of new maintenance procedures could also potentially become important sources of operational cost [36].

Finally, in considering increasing the MTOW we must also make the observation that such increases would be hard to justify if hybridisation was less profitable than, for example, increasing the payload capacity of the aircraft or adding more fuel tanks to extend range. Both are alternate changes that could yield increased profit if executed correctly and so airlines might simply ask “why increase my MTOW to add batteries when I could add more passengers and/or fuel?”

This factor largely depends on whether electricity prices at the point of purchase could remain considerably more competitive than kerosene long term. Both jet fuel and electricity prices are subject to significant fluctuations dependent on demand and geopolitical factors [13], [14], [15]. For example the 2022 Ukraine War had significant effects on oil prices which in turn both affected jet fuel price and, more significantly, UK electricity prices due to the country’s reliance on Russian natural gas [16].

Carbon/jet fuel taxation could provide an avenue to incentivise hybridisation, however attempts at this policy have led to increases in electricity prices in countries where the energy grid is heavily reliant on fossil fuels, for example, Australia [17].

At the time of writing, using sources [13] and [14], converting from USD to GBP ($1 = £0.74), using 159 litres per barrel, and 35 MJ/L for the volumetric energy density of jet fuel, the price of electricity in the UK per megajoule is 1.79x higher than that of jet fuel.

This must be contrasted with an important caveat however. Because of the improved efficiency of the power flow from the battery to the motor compared to the fuel to the motor (or shaft in the case of a parallel architecture), this figure *does not* truly represent the cost per unit of *useful* energy. Multiplying the above figure by $\frac{\eta_{fuel\ chain}}{\eta_{bat\ chain}}$, the cost of useful energy from the battery is 0.613x that for fuel, and so, in real terms, *electricity from the grid costs less than jet fuel per unit useful energy*.

This is the fundamental motivation behind hybridisation as a means of decarbonising the regional aviation sector, as reduced environmental impact could potentially go hand in hand with reduced operating costs at least in terms of energy consumption.

The cost of electricity is not negligible however, and the costs associated with new maintenance procedures, charging infrastructure and accelerated runway degradation need to be quantified before making a case to airlines and airports. The grid also needs to be adequately decarbonised for hybrid aircraft to be justified as an environmentally friendly solution.

To summarise, the viability of hybrid aircraft over the coming decade will be contingent on numerous factors. The development of lithium ion batteries that are safe and have much improved gravimetric energy density is crucial. The design of aircraft structures that can handle greater loads upon landing will be required if less mass is exhausted throughout flight. The costs of associated infrastructure must be appropriately quantified and managed. Finally, abundant, clean and cheap electricity must be available to airports.

References

[1] A. Batra, R. Raute, and R. Camilleri, “On the Range Equation for Hybrid-Electric Aircraft,” *Aerospace*, vol. 10, no. 8, p. 687, Aug. 2023, doi: https://doi.org/10.3390/aerospace10080687.

[2] “Purdue AAE Propulsion Website” *Purdue University*, 2019. https://engineering.purdue.edu/~propulsi/propulsion/index.html

[3] S. Yusuf, Setyo Hariyadi Suranto Putro, and Nyaris Pambudiyatno, “Numerical Simulation of Effect Modification of Single Slotted Flap on Wing Cessna C208B Grand Caravan for Aerodynamic Performance,” *ICATEAS 2022*, Feb. 2023, doi: https://doi.org/10.2991/978-94-6463-092-3_2.

[4] K. Sahin, Fazil Gomec, Murat Millidere, and J. Whidborne, “Aerodynamic Analysis of Saab 340B Aircraft with Data Fusion Implementation,” *AIAA SCITECH 2024 Forum*, Jan. 2024, doi: https://doi.org/10.2514/6.2024-2854.

[5] “FlyZero Zero Carbon Emission Aircraft Concepts” *Aerospace Technology Institute* 2022. https://www.ati.org.uk/wp-content/uploads/2022/03/FZO-AIN-REP-0007-FlyZero-Zero-Carbon-Emission-Aircraft-Concepts.pdf

[6] “Caravan Brochure.” *Textron Aviation*, 2025. https://cessna.txtav.com/-/media/cessna/files/brochures/turboprop/caravan_brochure.pdf

[7] “Saab340B/Bplus. ” *Saab Aircraft Leasing*, 2009. https://lipicanaer.eu/wp-content/uploads/2020/01/340B_easa.pdf

[8] “ATR 72-600.” *ATR Aircraft*, 2022. https://www.atr-aircraft.com/wp-content/uploads/2022/06/ATR_Fiche72-600-3.pdf?_gl=1

[9] G. Punzo, “AER11002: Introduction to Aerospace: Design, Build and Test Lecture Notes”, *University of Sheffield*, 2024.

[10] Y. Nie, P. Ko, and R. Drummond, “Optimal Flight Trajectories of Hybrid Electric Aircraft with In-Flight Charging,” *2022 European Control Conference (ECC)*, pp. 218–223, Jun. 2024, doi: https://doi.org/10.23919/ecc64448.2024.10590832.

[11] “CAT.OP.MPA.151 Fuel policy — alleviations,” *Civil Aviation Authority*, 2024. https://regulatorylibrary.caa.co.uk/965-2012/Content/Regs/06780_CATOPMPA151_Fuel_policy_alleviations.htm

[12] D. Chen, Q. Luo, M. Meng, Q. Li, and G. Sun, “Low velocity impact behavior of interlayer hybrid composite laminates with carbon/glass/basalt fibres,” *Composites Part B: Engineering*, vol. 176, p. 107191, Nov. 2019, doi: https://doi.org/10.1016/j.compositesb.2019.107191.

[13] International Air Transport Association, “Jet Fuel Price Monitor,” *IATA*, 2025. https://www.iata.org/en/publications/economics/fuel-monitor/

[14] Trading Economics, “United Kingdom Electricity Price - 2022 Data - 2013-2021 Historical - 2023 Forecast,” *tradingeconomics.com*, 2022. https://tradingeconomics.com/united-kingdom/electricity-price

[15] McKinsey & Company, “Why rising fuel prices might not be as bad for the airline sector as it seems,” *McKinsey & Company*, Jul. 15, 2022. https://www.mckinsey.com/industries/travel/our-insights/why-rising-fuel-prices-might-not-be-as-bad-for-the-airline-sector-as-it-seems

[16] P. Bolton, “Gas and electricity prices during the ‘energy crisis’ and beyond,” House of Commons Library, London, United Kingdom, Feb. 2025. Accessed: Apr. 27, 2025. [Online]. Available: https://researchbriefings.files.parliament.uk/documents/CBP-9714/CBP-9714.pdf

[17] J. B. Wong and Q. Zhang, “Impact of carbon tax on electricity prices and behaviour,” *Finance Research Letters*, vol. 44, p. 102098, May 2021, doi: https://doi.org/10.1016/j.frl.2021.102098.

[18] G. Pawelec, “Comparative report on alternative fuels for ship propulsion,” Interreg North-West Europe, Lille, France, Jul. 2020. Accessed: Apr. 27, 2024. [Online]. Available: https://vb.nweurope.eu/media/14694/210225_h2ships_t232_compassesmtaltfuels-02.pdf

[19] M. F. Rojas-Michaga *et al.*, “Sustainable aviation fuel (SAF) production through power-to-liquid (PtL): A combined techno-economic and life cycle assessment,” *Energy Conversion and Management*, vol. 292, p. 117427, Sep. 2023, doi: https://doi.org/10.1016/j.enconman.2023.117427.

[20] “Aircraft Concepts,” *DLR EXACT*, Mar. 04, 2024. https://exact-dlr.de/aircraft-concepts/ (accessed Apr. 27, 2025).

[21] “Home | HERA,” *Project HERA*, 2025. https://project-hera.eu/home (accessed Apr. 27, 2025).

[22] Airbus, “EcoPulse results suggest a bright future for hybrid-electric aviation,” *Airbus*, Jan. 27, 2025. https://www.airbus.com/en/newsroom/stories/2025-01-ecopulse-results-suggest-a-bright-future-for-hybrid-electric-aviation

[23] Heart Aerospace, “ES-30 | Heart Aerospace.” https://heartaerospace.com/es-30/

[24] Souha Elmousadik, Vladimir Ridard, N. Sécrieru, Aleksandar Joksimovic, C. Maury, and X. Carbonneau, “New Preliminary Sizing Methodology for a Commuter Airplane with Hybrid-Electric Distributed Propulsion,” *HAL Open Science*, pp. 1–11, Oct. 2018, doi: https://hal.science/hal-01994750.

[25] “Aircraft Configurations,” *NASA*, Feb. 20, 2025. https://www.nasa.gov/eap-aircraft-concepts/aircraft-configurations/

[26] F. M. N. U. Khan, M. G. Rasul, A. S. M. Sayem, and N. Mandal, “Maximizing energy density of lithium-ion batteries for electric vehicles: A critical review,” *Energy Reports*, vol. 9, no. 11, pp. 11–21, Oct. 2023, doi: https://doi.org/10.1016/j.egyr.2023.08.069.

[27] CATL, “CATL launches condensed battery with an energy density of up to 500 Wh/kg, enables electrification of passenger aircrafts,” *CATL*, Apr. 19, 2023. https://www.catl.com/en/news/6015.html

[28] “Wright Batteries,” *Wright Electric* https://www.weflywright.com/battery-launch

[29] J. D. Gotz, M. A. S. Teixeira, F. C. Corrêa, E. R. Viana, A. A. Badin and M. Borsato, "The Influence of Overcharging and Over-Discharging on the Capacity Degradation of Lithium-Ion Batteries," *2024 IEEE Vehicle Power and Propulsion Conference (VPPC)*, Washington, DC, USA, 2024, pp. 1-6, doi: 10.1109/VPPC63154.2024.10755337.

[30] Y. Zheng *et al.*, “Influence of over-discharge on the lifetime and performance of $LiFePO_4$/graphite batteries,” *RSC Advances*, vol. 6, no. 36, pp. 30474–30483, 2016, doi: https://doi.org/10.1039/c6ra01677d.

[31] “Wright WM2500 Is Assembled and Spinning Freely!,” *Wright Electric*, 2025. https://www.weflywright.com/blog-posts/0dbba70dc4-a2c21 (accessed Apr. 28, 2025).

[32] “ZA2000,” *ZeroAvia*. https://zeroavia.com/za2000/

[33] L. Sampaio and J. Costa, “Electric Taxiing System. Kinetic Energy Recovery System as an Electric Taxiing Solution: Economic and environmental analysis: Phenom 300 case study,” *Journal of the Air Transport Research Society*, vol. 3, p. 100037, Aug. 2024, doi: https://doi.org/10.1016/j.jatrs.2024.100037.

[34] B. Rowland, “How Much Fuel Does a Plane Use During Flight?,” *OAG*, Feb. 03, 2022. https://www.oag.com/blog/which-part-flight-uses-most-fuel

[35] J. M. Low, R. Stuart Haszeldine, and Julien Mouli-Castillo, “The hidden cost of road maintenance due to the increased weight of battery and hydrogen trucks and buses—a perspective,” *Clean Technologies and Environmental Policy*, vol. 25, no. 3, pp. 757–770, Dec. 2022, doi: https://doi.org/10.1007/s10098-022-02433-8.

[36] Nicolò Avogadro and R. Redondi, “Demystifying electric aircraft’s role in aviation decarbonization: Are first-generation electric aircraft cost-effective?,” *Transportation Research Part D Transport and Environment*, vol. 130, pp. 104191–104191, May 2024, doi: https://doi.org/10.1016/j.trd.2024.104191.

Appendix: MATLAB Code

Code for plotting Figures 1 and 2

```
%physical constants
g=9.81;

nPhiPoints = 1001;
nMassEnergyPoints = 1001;

%aircraft params

%efficiencies
PSFC = 0.0000001113484452;

liftDragRatio=13.5;

etaProp=0.8;
etaTurbine = 0.35;
etaGenerator = 0.98;
etaMotor = 0.9;
etaGearbox = 0.95;

etaFuelChain = etaTurbine*etaGearbox*etaGenerator*etaMotor*etaProp;
etaBatChain = etaGearbox*etaMotor*etaProp;

%mission requirements
massPayload=1200;
rangeLowerBound=500 *10^3;

%masses

massOperatingEmpty=2145;


maxMTOW=1.75*3629;

%specific energies/consumption
eBat=0.8*500*3600;
eFuel = 43.1*10^6;

%bounds on fuel mass
deltaMConventional= 3629*(1-exp(-
(rangeLowerBound*g*PSFC)/(etaProp*liftDragRatio)));

%the energy mass must be at least equal to the conventional fuel deltaM
%but must not exceed MTOW-payload-oem

%dependent variables
phi=linspace(0,1,nPhiPoints);
massEnergy = linspace(deltaMConventional,(maxMTOW-massOperatingEmpty-
massPayload),nMassEnergyPoints)';


%independent variables
massFuel = (((1-phi).*eBat.*massEnergy)./(phi.*eFuel+(1-phi).*eBat));
normalisedFuelMass = (1./deltaMConventional).*massFuel;


MTOW=massPayload+massOperatingEmpty+massEnergy;
```

```
normalisedMTOW = MTOW./3629;

range = (1/g).*liftDragRatio.*( etaFuelChain.*eFuel.*log((MTOW)./(MTOW-massFuel))
+ etaBatChain.*(eBat.*(massEnergy-massFuel))./(MTOW-massFuel));

%normalisedFuelMass = phi.*ones([100 1]);

%two criteria for feasibility
%1. consumed fuel mass is lower than a conventional equivalent
%2. range can be achieved with given energy mix

%remove all points that have a percent fuel saving less than 0 or that
%don't meet the range requirement
for i = 1:nPhiPoints
    for  j = 1:nMassEnergyPoints
        if (normalisedFuelMass(j,i) > 1)
           normalisedFuelMass(j,i) = NaN;
           %fprintf("Target: %f\tActual:
%f\n\n",range,modifiedBreguetRange(phi(i), massEnergy(j), etaFuelChain,
etaBatChain, liftDragRatio, eBat, eFuel, g,
(massEnergy(j)+massPayload+massOperatingEmpty)));
        elseif (range(j,i) < rangeLowerBound)
        %if (range(j,i) < rangeLowerBound)
            normalisedFuelMass(j,i) = NaN;
            %fprintf("Target: %f\tActual:
%f\n\n",range,modifiedBreguetRange(phi(i), massEnergy(j), etaFuelChain,
etaBatChain, liftDragRatio, eBat, eFuel, g,
(massEnergy(j)+massPayload+massOperatingEmpty)));
        end
    end
end

percentFuelSaving = (1-normalisedFuelMass)*100;

figure(1);
surf(phi,normalisedMTOW,percentFuelSaving,"EdgeColor","none");
xlabel("Degree of Hybridisation");
ylabel("Normalised MTOW");
zlabel("Percent Fuel Saving (%)");
view(3);
saveas(figure(1),"Figures\Surface\PercentFuelSaving","jpg")

figure(2);
surf(phi,normalisedMTOW,range*10^-3,"EdgeColor","none");
xlabel("Degree of Hybridisation");
ylabel("Normalised MTOW");
zlabel("Range (km)");
saveas(figure(2),"Figures\Surface\Range","jpg")

% figure(3);
% contour(phi,massEnergy,range*10^-3);
% xlabel("Degree of Hybridisation");
% ylabel("Mass of Energy (kg)");
% zlabel("Range (km)");

minFC = min(min(normalisedFuelMass));
indexOfMinFC = find(normalisedFuelMass==minFC);
```

```
fprintf("Minimum normalised fuel consumption: %f\nAchieved at phi=%f Energy
Storage Mass = %f kg\n",minFC, phi(fix(indexOfMinFC/nPhiPoints)),
massEnergy(mod(indexOfMinFC,nMassEnergyPoints)));

% function R = modifiedBreguetRange(phi, massEnergy, etaFuelChain, etaBatChain,
liftDragRatio, eBat, eFuel, g, MTOW)
%     massFuel = ((1-phi)*eBat*massEnergy)/(phi*eFuel+(1-phi)*eBat);
%     %massBat = massEnergy-massFuel;
%
%     R=(1/g)*liftDragRatio*(etaFuelChain*eFuel*log(MTOW/(MTOW-massFuel) +
etaBatChain*(eBat*(massEnergy-massFuel))/(MTOW-massFuel)) );
% end
```

Code for Plotting Figures 4-6 a-d

```
displayOutput = false;

%physical constants
g=9.81;
%aircraft params

%efficiencies
PSFC = [0.0000001113484452 0.00000007789322188 0.0000000790759823];

liftDragRatio=[13.5 14 16.8];

etaProp=0.8;
etaTurbine = 0.35;
etaGenerator = 0.98;
etaMotor = 0.9;
etaGearbox = 0.95;

etaFuelChain = etaTurbine*etaGearbox*etaGenerator*etaMotor*etaProp;
etaBatChain = etaGearbox*etaMotor*etaProp;

%mission requirements
massPayload=[1200, 3298, 7400];

%masses

massOperatingEmpty=[2145 8620 13600];

aircraftMTOW=[3629 13155 23000];

aircraftNames = ["Cessna 208 Caravan" "SAAB 340B" "ATR72-600"];

%specific energies/consumption
eBat = 0.8*3600*linspace(300,900,4);
eFuel = 43.1*10^6;



%the energy mass must be at least equal to the conventional fuel deltaM
%but must not exceed MTOW-payload-oem

%dependent variables
nRangePoints = 701;


for i =1:3
    mkdir(strcat("Figures\",aircraftNames(i)))
end


for q = 1:4
    for i=1:3
        rangeConventional =
etaProp*liftDragRatio(i)*log(aircraftMTOW(i)/(massPayload(i)+massOperatingEmpty(i)
))/(g*PSFC(i));
        rangeLowerBound=linspace(0,rangeConventional,nRangePoints);
        for MTOWMultiplier = linspace(1,2,5)
            for j = 1:nRangePoints
```

```
                %bounds on fuel mass
                deltaMConventional=(aircraftMTOW(i))*(1-exp(-
g*PSFC(i)*rangeLowerBound(j)/(liftDragRatio(i)*etaProp)));

                maxMTOW=MTOWMultiplier*aircraftMTOW(i);
                massEnergy = maxMTOW - massPayload(i) - massOperatingEmpty(i);

                phiUpper = 1;
                phiLower = 0;

                for k=1:16
                    phi = (phiUpper+phiLower)/2;
                    massFuel = (((1-phi).*eBat(q).*massEnergy)./(phi.*eFuel+(1-
phi).*eBat(q)));
                    range = (1/g)*liftDragRatio(i)*(
etaFuelChain*eFuel*log((maxMTOW)/(maxMTOW-massFuel)) +
etaBatChain*(eBat(q)*(massEnergy-massFuel))/(maxMTOW-massFuel));
                    if range>=rangeLowerBound(j)
                        phiLower=phi;
                    elseif range<rangeLowerBound(j)
                        phiUpper = phi;
                    end
                    normalisedFuelMass = (1./deltaMConventional).*massFuel;
                end

                if displayOutput
                    fprintf("Normalised Fuel Consumption Minimised at
phi=%f\n",phi);
                    fprintf("\tNFC = %f\n",normalisedFuelMass);
                    fprintf("\tRange = %.0f km\n",range*10^-3);
                end

                percentFuelSaving(j)=(1-normalisedFuelMass)*100;

            end
            figure(3*(q-1)+i);
            plot(rangeLowerBound*10^-
3,percentFuelSaving,"DisplayName",strcat("MTOW = ",string(MTOWMultiplier),"x"));
            xlabel("Range (km)")
            ylabel("Percent Fuel Saving (%)");
            yline(0,"--",'HandleVisibility','off');
            hold on
        end
        title(strcat(aircraftNames(i), " Battery Energy Density =
",string(eBat(q)/(3600*0.8)),"Wh/kg"));
        legend();
        saveas(figure(3*(q-1)+i),strcat("Figures\",aircraftNames(i),"\Battery
Energy Density = ",string(eBat(q)/(3600*0.8))),"png");
    end
end
```